

July 1998

IFUP-TH 27/98  
hep-lat/9807019

# Wilson loop distributions, higher representations and centre dominance in $SU(2)$

**P.W. Stephenson**

Dipartimento di Fisica dell'Università and INFN,  
I-56100 Pisa, Italy  
Email: `pws@ibmth.df.unipi.it`

## Abstract

To help understand the centre dominance picture of confinement, we look at Wilson loop distributions in pure  $SU(2)$  lattice gauge theory. A strong coupling approximation for the distribution is developed to use for comparisons. We perform a Fourier expansion of the distribution: centre dominance here corresponds to suppression of odd terms beyond the first. The Fourier terms correspond to  $SU(2)$  representations; hence Casimir scaling behaviour leads to centre dominance. We examine the positive plaquette model, where only thick vortices are present. We show that a simple picture of random, non-interacting centre vortices gives a string tension about  $3/4$  of the measured value. Finally, we attempt to limit confusion about the adjoint representation.

PACS codes: 11.15.Ha, 12.38.Aw, 12.38.Gc

Keywords:  $SU(2)$ , lattice, confinement, centre vortices, representations

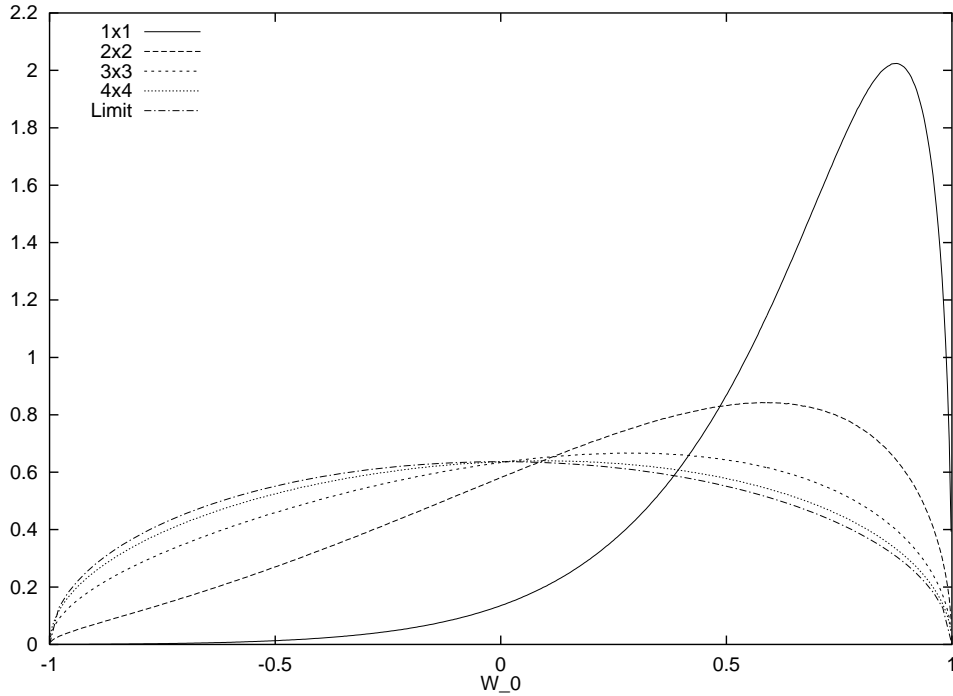


Figure 1: Monte Carlo distribution of Wilson loops on a  $12^4$  lattice at  $\beta = 2.5$ , showing also the limit of the distribution for large loops. The area under each curve is normalised to unity. On this scale errors are negligible.

## 1 INTRODUCTION

Recently the idea, originally proposed some time ago [1, 2, 3], that confinement in gauge theories can be considered as an effect related to the centre  $Z(N)$  of the gauge group  $SU(N)$  has been undergoing a revival [4, 5, 6, 7]. Not the least of this has been the demonstration [7] that if one replaces the values of Wilson loops with their signs alone (i.e. the centre  $Z(2)$ ) the heavy quark potential in  $SU(2)$ , which is now very accurately known [8], can be essentially *completely* reproduced. This is a spectacular — and gauge invariant — demonstration that something is right about this hypothesis; it is, however, far from a demonstration that centre vortices are responsible for confinement.

The key part of the argument for  $Z(2)$  to be an ingredient in confinement is that there are ‘thick’ centre vortices, associated with the quotient group  $SU(2)/Z(2) \cong SO(3)$ , which pierce Wilson loops; their physical effect depends on how many vortices, modulo 2, pierce a given area. There are also ‘thin’ vortices associated with  $Z(2)$ , which appear as chains of negative plaquettes; to create these requires an action proportional to the number of flipped plaquettes, so these will not survive in the continuum limit. By contrast, the thick vortices show up only in larger Wilson loops, which may be negative while still surrounding only positive plaquettes, and do survive in the continuum limit; they are topological in nature, related to the fact that  $SU(2)/Z(2)$  is not simply connected and indeed has a  $Z(2)$  homotopy. (For simplicity, we have here ignored hybrid vortices, which combine the two effects.) We shall return to the distinction between  $Z(2)$  and  $SU(2)/Z(2)$  effects towards the end of the article because, as emphasised in ref. [7] where this mechanism is described in more detail, it is important and has caused much confusion.

We have specialised to  $SU(N)$  for  $N = 2$  since the arguments are expected to extend to higher  $N$  via the centre  $Z(N)$ , though of course this needs to be checked explicitly. We are also ignoring the effects of fermions in the vacuum.

Because  $Z(2)$  commutes with all elements of the gauge group, the sign of any Wilson loop in the fundamental representation of  $SU(2)$  must be determined by the combined effect of thin and thick vortices: the total of these objects passing through the loop determines whether the loop is positive (even number of vortices) or negative (odd number). In an attempt to see how this appears, we can look at the distribution of the trace of the Wilson loop, as generated by a Monte Carlo simulation. Note we are looking at the distribution of individual, not average, Wilson loops. One such set, taken from 10,000 configurations of a  $12^4$  lattice at  $\beta = 2.5$ , is shown in fig. 1. It is clear that it changes smoothly from the highly asymmetric shape of the plaquette action to some limiting distribution for large loops. It is less clear how the Wilson loop expectation value  $\langle W_0 \rangle$ , which is the first moment of the distribution, behaves; nor is it clear where the special role of the sign of the loop comes from.

This paper attempts to shed some light on these matters. As the behaviour of the distribution is largely unfamiliar territory, we first perform a calculation using a simple approximation: we are not able to calculate the raw distribution, but we are able to see how it develops for larger loops. The expectation value in this approximation has the leading order strong coupling behaviour.

We shall proceed as follows: first (section 2) we shall give a few basic home truths about Wilson loops. Next (section 3), we shall look at the approximation that all loops are uncorrelated, corresponding to strong coupling; in section 4 we discuss the centre dominance picture in the same spirit, where we also explicitly show the connection between the shape of the distribution, irreducible representations of  $SU(2)$  and the phenomenon of centre dominance. Then we make some remarks about centre-projected vortices, the positive plaquette model, the adjoint representation, and show how a gas of non-interacting  $Z(2)$  vortices gives exact area law confinement. In the last section we summarise these results concisely.

Section 3 can safely be missed out by anyone not interested in the details of the distributions of uncorrelated Wilson loops. Of the formalism in that section we shall only use the formula relating the distributions for loops of areas  $A$  and  $2A$ , eqn. (14), and its extension to arbitrary multiples of  $A$ . The main physical discussion is in section 4.

## 2 WILSON LOOP DISTRIBUTIONS

We shall start by assuming the standard Wilson lattice gauge theory in  $SU(2)$ . We parametrise an open Wilson loop (i.e. the  $SU(2)$  element representing the loop, where no trace has been taken) as

$$W \equiv W_0 \mathbf{1}_2 + i\sigma \cdot \mathbf{W}, \quad W_0^2 + W_1^2 + W_2^2 + W_3^2 = 1. \quad (1)$$

We now consider the distribution, the word being used in the sense of a Monte Carlo calculation: we have a large number of configurations, and consider the spread of values for all Wilson loops of a given shape on all lattices. Of course, we could equally well talk in terms of contributions to the path integral, where, because of the importance sampling built into the Monte Carlo simulations, the exponential factor is included and there is a uniform measure; this is entirely equivalent. However, the statistical language fits well here where we use actual Monte Carlo data for comparison. The distribution contains all the gauge invariant information about the loops, including the expectation values of the loops in all representations. Indeed, in a quantum theory it is natural to consider this distribution as the basic quantity.

The first matter of interest is the limiting large loop distribution apparent in fig. 1. This can easily be calculated. Given the short range behaviour of the force, for sufficiently large loops different parts of the loop are physically unconnected with one another. The lack of any overall correlation means the loops are random: the distribution corresponds to a random walk by  $W_i$  over the 3-sphere of the gauge manifold, so we simply need to calculate the fraction of the surface available at a given  $W_0$  with the other co-ordinates fixed. The probability that  $W_0$  lies in a certain range is

$$\rho_l(W_0) dW_0 = S_0 ds_0 / S, \quad (2)$$

where here, as throughout, we use the symbol  $\rho$  for the distribution and the suffix  $l$  indicates the limiting distribution,  $S_0$  is the 2-surface for a given  $W_0$ , while between  $W_0$  and  $W_0 + dW$  a distance  $ds_0$  is covered on the surface of the 3-sphere with the other co-ordinates held constant, and  $S$  is the total surface area of the 3-sphere. Basic geometry gives

$$\rho_l(W_0) dW_0 = \frac{4\pi(1 - W_0^2)}{2\pi^2} \frac{dW_0}{(1 - W_0^2)^{1/2}} = \frac{2}{\pi} (1 - W_0^2)^{1/2} dW_0. \quad (3)$$

This is the lowest curve in fig. 1 and clearly fits the part. Indeed, loops larger than  $4 \times 4$  are so close to this that they have been omitted for clarity. Later, we will see that this curve corresponds to the identity representation of  $SU(2)$ ; it will then be obvious that convergence to this limit is inevitable provided that all  $j = 1/2$  and higher representation Wilson loops decay monotonically.

The loop distribution in figure 1 is smooth and we would expect to be able to expand it in a Fourier series. We will pick the units  $W_0 \equiv \sin \frac{\phi}{2}$ , where  $-\pi \leq \sin \frac{\phi}{2} \leq \pi$  so that the terms are orthogonal on the range of values of  $W_0$ . However, our expansion is not quite standard; we use our freedom to expand the even and odd parts separately to write,

$$\rho_{A_d}(W_0) \equiv \rho_{A_d}(\sin \frac{\phi}{2}) = \sum_{n=1}^{\infty} (a_n \cos(n - \frac{1}{2})\phi + b_n \sin n\phi). \quad (4)$$

The difference from the usual Fourier series is that this form satisfies the boundary condition that the function vanishes at  $\phi = \pm\pi$ . The basis corresponds to the eigenfunctions of the self-adjoint linear equation

$$\frac{d^2\rho}{d\phi^2} + \nu^2\rho = 0 \quad (5)$$

with those boundary conditions, so that orthogonality (which may easily be checked) and completeness are guaranteed by Sturm-Liouville theory. We will later show that there is a one-to-one correspondence between these terms and the expectation value in irreducible representations of the gauge group; this is why we have picked this form. This means that any distribution which does not vanish at the boundary does not have an interpretation in terms of the underlying group theory. The large area limit is already visible as the  $a_1$  term.

As a final piece of preparatory formalism, we also calculate the average Wilson loop in the fundamental representation from the Fourier series; this is

$$\begin{aligned} \langle W_0 \rangle &= \int_{-1}^1 \rho_{A_d}(W_0) W_0 dW_0 = \int_{-\pi}^{\pi} \rho_{A_d}(W_0) \sin \frac{\phi}{2} \cos \frac{\phi}{2} d\phi/2 \\ &= (1/4) \int_{-\pi}^{\pi} (b_1 \sin \phi) \sin \phi d\phi = \frac{\pi b_1}{4}, \end{aligned} \quad (6)$$

since by orthogonality only the first odd term in the expansion survives. Later we will generalise this formula to all representations.

### 3 THE UNCORRELATED LOOP APPROXIMATION

We now claim that due to gauge invariance we can always write an individual Wilson loop (the qualification is important) chosen from the distribution as

$$W \equiv W_0^2 + \sqrt{1 - W_0^2} \sigma \cdot \mathbf{e}_r, \quad (7)$$

where  $\mathbf{e}_r$  is a unit vector in a random direction in the 3-space inhabited by  $\mathbf{W}$ . This is essentially a consequence of Elitzur's theorem. To see this, consider any Wilson loop of a given shape with its opening at a particular point on a lattice. If the distribution of  $\mathbf{W}$  is not as shown, then there

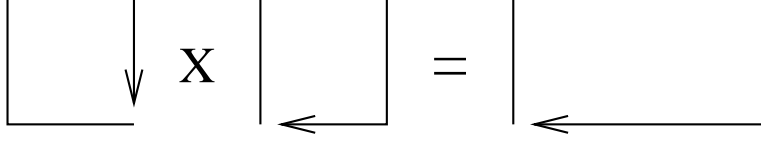


Figure 2: Multiplication of adjacent Wilson loops. We can move the opening using a gauge transformation and hence create loops of any size in this fashion.

must be some preferred direction(s) for  $\mathbf{W}$ . However, we can perform a local gauge transformation at the site of the opening. It is easy to see that this leaves  $W_0$  invariant, while rotating  $\mathbf{W}$  to an arbitrary angle. As we have complete freedom to do this, with the single exception that rotations of Wilson loops with their openings on the same site are correlated, we can move the preferred direction of  $\mathbf{W}$ . (We can avoid the exception here by simply considering only sets of translated Wilson loops without rotations, which gives a perfectly valid distribution.) Thus there is no preferred direction after all, and the distribution is the one claimed.

We now take two Wilson loops,  $W^1(A)$  and  $W^2(A)$ , of the same shape and area  $A$ , but chosen in such a way that their opening lies on the same site, fig. 2. It will also be convenient to choose rectangular loops with a side in common traversed in such a way that this cancels out in the product of the loops. Thus we produce a Wilson loop of twice the area. The  $W_0$  element of this loop, by the standard  $SU(2)$  multiplication rule, is:

$$W_0(2A) = W_0^1(A)W_0^2(A) - (1 - W_0^1(A)^2)^{1/2}(1 - W_0^2(A)^2)^{1/2}\cos\xi, \quad (8)$$

where  $\cos\xi \equiv \mathbf{e}_r^1 \cdot \mathbf{e}_r^2$ ;  $\xi$  is the angle between the two unit three vectors in the directions  $\mathbf{W}^1(A)$  and  $\mathbf{W}^2(A)$ .

The correlations between the diagonal elements  $W_0^i(A)$  in eqn. (8) together with the angle  $\xi$  contain all the information about correlations between adjacent loops; without them we simply have loops from a random distribution multiplied together. If we were to go on and consider larger loops still, we would have to consider the cumulative effect of these correlations on the larger loops, and the expressions would rapidly become unmanageable.

Instead, we make the approximation that both the angular and the diagonal correlations are negligible for loops larger than some area  $A = A_d$ . We shall later see explicitly that this gives the leading strong coupling value for  $\langle W_0 \rangle$ , although in our case expanded in terms of smaller Wilson loops rather than the coupling itself. That such behaviour is expected is due to the random nature of the choice of loops from the distribution.

A random distribution for  $\cos\xi$  is simply a flat distribution, which follows from the fact that the usual measure for the polar angle on a 2-sphere (here the one containing  $\mathbf{e}_r^i$ ) is  $\sin\xi d\xi = d\cos\xi$ . We are assuming, however, that the loop distribution  $\rho(W_0)$  itself has not reached the large area limit. The formula (8) can now be used to multiply loops of different sizes, and we can build up larger Wilson loops by repeated application. Moving the opening in the Wilson loop simply corresponds to a gauge transformation, leaving the only remaining variable  $W_0$  invariant, so there is no difficulty in constructing Wilson loops of any area which is a multiple of  $A_d$  by this method.

Our procedure is to take the measured Monte Carlo distribution of  $W_0$  on loops of area  $A = A_d$  as our input and hence use the approximation to calculate the distribution of Wilson loops for larger areas. In our examples, we shall in fact start from the plaquette, i.e. take  $A_d = 1$  in lattice units and the measured plaquette distribution, but this is not forced on us. This method is obviously something of a hybrid, since the initial distribution includes all correlations, but it will allow us to perform explicit calculations using the loop distribution. Further, we will be able to predict the behaviour, starting from the appropriate expectation value for the plaquette, in every representation of the gauge group.

### Calculation of the product distribution

Suppose that the probability distribution of  $W_0$  for loops of the initial size  $A_d$  is given by  $\rho_{A_d}(W_0)dW_0$ , normalised so that the integral between  $W_0 = -1$  and  $1$  is unity. To produce the distribution of larger loops we must integrate over the smaller ones, using the equation (8) as a constraint. It will be helpful at this point to change to angular variables: take  $W_0(2A_d) \equiv \cos \Theta$ , where  $0 \leq \Theta \leq \pi$ , and likewise  $W_0^i(A_d) \equiv \theta_i$  for  $0 \leq \theta_i \leq \pi$ . The new distribution is given by

$$\rho_{2A_d}(W_0)dW_0 = \frac{1}{2} \int \int \rho_{A_d}(\cos \theta_1) \rho_{A_d}(\cos \theta_2) \sin \theta_1 d\theta_1 \sin \theta_2 d\theta_2 \sin \xi d\xi, \quad (9)$$

where the extra factor of  $1/2$  in eqn. (9) has appeared because in covering the full range of  $\theta_1$  and  $\theta_2$  we cover the  $\Theta$  range exactly twice. This can be seen by simultaneously exchanging  $\theta_1 \leftrightarrow \pi - \theta_1, \theta_2 \leftrightarrow \pi - \theta_2$  in eqn. (10), which leaves  $W_0$  invariant.

The range in this notation is taken from eqn. (8) which becomes

$$W_0 \equiv \cos \Theta = \cos \theta_1 \cos \theta_2 - \sin \theta_1 \sin \theta_2 \cos \xi. \quad (10)$$

Note that with the correct normalisation of  $\rho_{A_d}(\cos \theta)$ , the new distribution will also be correctly normalised, i.e.  $\int \rho_{2A_d}(W_0)dW_0 = 1$ , regardless of the form of  $\rho$ ; this is nothing more than a basic consistency condition for the integrals we are performing.

We remove  $d\xi$  from eqn. (9) using eqn. (10),  $\sin \theta_1 \sin \theta_2 \sin \xi d\xi = dW_0$ , giving

$$\rho_{2A_d}(\cos \Theta) = \frac{1}{2} \int \int_{\text{constraint}} \rho_{A_d}(\cos \theta_1) \rho_{A_d}(\cos \theta_2) d\theta_1 d\theta_2 \quad (11)$$

with the constraint of eqn. (10). The considerable simplification due to the approximation that  $\cos \xi$  has a random distribution is now evident. We now have to put this in terms of explicit limits for  $\theta_1$  and  $\theta_2$ . The limits of the  $\theta_1$  integration for fixed  $\theta_2$  are where  $\cos(\theta_1 \pm \theta_2) = \cos \Theta$ , with the limits smoothly becoming equal as  $\theta_2 \rightarrow 0$ . One finds

$$\begin{aligned} 2\rho_{2A_d}(\cos \Theta) &= \int_0^\Theta \rho_{A_d}(\cos \theta_2) d\theta_2 \int_{\Theta-\theta_2}^{\Theta+\theta_2} \rho_{A_d}(\cos \theta_1) d\theta_1 \\ &+ \int_\Theta^{\pi-\Theta} \rho_{A_d}(\cos \theta_2) d\theta_2 \int_{\theta_2-\Theta}^{\theta_2+\Theta} \rho_{A_d}(\cos \theta_1) d\theta_1 \\ &+ \int_{\pi-\Theta}^\pi \rho_{A_d}(\cos \theta_2) d\theta_2 \int_{\theta_2-\Theta}^{2\pi-\Theta-\theta_2} \rho_{A_d}(\cos \theta_1) d\theta_1. \end{aligned} \quad (12)$$

This is written in the form appropriate for  $0 \leq \Theta \leq \pi/2$ . For  $\pi/2 \leq \Theta \leq \pi$ , the  $\Theta$ 's in the  $\theta_2$  integrals are replaced by  $\pi - \Theta$ , and the range for the central  $\theta_1$  integration becomes  $[\Theta - \theta_2, 2\pi - \Theta - \theta_2]$ . It is easy to show by formal manipulation of the limits that these two integrals are in fact identical, as they should be.

We can also now confirm that using the limiting distribution  $\rho_{A_d}(\cos \theta) = (2/\pi) \sin \theta$  as an input produces the same distribution for  $\rho_{2A_d}(\cos \Theta)$ , as expected.

### Evaluation of the integral

We shall now evaluate the integral eqn. (12) for a general distribution. It will be convenient to change variables once again to the  $\phi$  used in the Fourier series (4), even though the integral is slightly more messy in this form, writing  $W_0 \equiv \cos \theta \equiv \sin \frac{\phi}{2}$ . The integral becomes, with a change

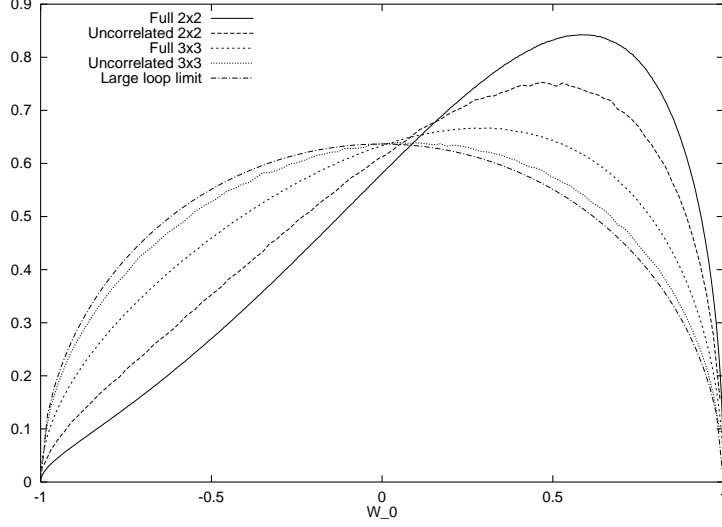


Figure 3: Comparison of Wilson loop distributions from Monte Carlo and those from the uncorrelated loop approximation (where the noise is clearly visible). The measured plaquette distribution has been used as a starting point for the latter.

of notation to  $W_0(2A_d) \equiv \sin \frac{\Phi}{2}$ ,  $W_0^1(A_d) \equiv \sin \frac{\phi_1}{2}$ ,  $W_0^2(A_d) \equiv \sin \frac{\phi_2}{2}$ :

$$\begin{aligned}
8\rho_{2A_d}(\sin \frac{\Phi}{2}) &= \int_{-\pi}^{-\Phi} \rho_{A_d}(\sin \frac{\phi_2}{2}) d\phi_2 \int_{-\pi-\Phi-\phi_2}^{\pi-\Phi+\phi_2} \rho_{A_d}(\sin \frac{\phi_1}{2}) d\phi_1 \\
&\quad + \int_{-\Phi}^{\Phi} \rho_{A_d}(\sin \frac{\phi_2}{2}) d\phi_2 \int_{-\pi+\Phi+\phi_2}^{\pi-\Phi+\phi_2} \rho_{A_d}(\sin \frac{\phi_1}{2}) d\phi_1 \\
&\quad + \int_{\Phi}^{\pi} \rho_{A_d}(\sin \frac{\phi_2}{2}) d\phi_2 \int_{-\pi+\Phi+\phi_2}^{\pi+\Phi-\phi_2} \rho_{A_d}(\sin \frac{\phi_1}{2}) d\phi_1,
\end{aligned} \tag{13}$$

which is in the form for  $0 \leq \Phi \leq \pi$ .

We are now in a position to insert the Fourier expansion of eqn. (4) into eqn. (13). After some tedious algebra best left to computers we obtain,

$$\rho_{2A_d}(\sin \frac{\Phi}{2}) = \sum_{n=1}^{\infty} \frac{(-1)^{n-1} \pi}{4} \left( \frac{a_n^2}{n - \frac{1}{2}} \cos(n - \frac{1}{2})\Phi + \frac{b_n^2}{n} \sin n\Phi \right). \tag{14}$$

Both odd and even sets of terms remain separate; as we have already hinted, this is no coincidence.

The relationship between  $b_1$  and the loop expectation value was given in eqn. (6). We now read off the coefficient of  $\sin \Phi$  which is  $\pi b_1^2/4$ , hence the new expectation value is  $(\pi b_1/4)^2$ . Because the terms in the expansion remain separate, we can immediately extend the result to  $N$  multiplications and a loop size  $A \equiv N + 1$ ,

$$\langle W_0(A) \rangle = (\pi b_1/4)^{1+N} = W_0(1)^A, \tag{15}$$

an area law behaviour with string tension  $-\log(W_0(1))$ .

Eqn. (15) is equivalent to the lowest order strong coupling result, even though in this case no mention of the coupling has been made; indeed, it is renormalised due to the fact that we start from the physical plaquette rather than the strong coupling prediction, although the behaviour for larger loops in terms of the plaquette is the same.

In fig. 3, we compare distributions from uncorrelated loops with the measured values taken from fig. 1; as already stated, we have started from the measured plaquette distribution to generate the uncorrelated loop distributions. The multiplications in this case were done by Monte

Carlo integration of the rule (9), which was rather more convenient than applying the analytical formulae, thus accounting for the noise in this distribution. Not surprisingly, we immediately see the measured shape start to diverge from the uncorrelated loop shape.

## 4 CENTRE DOMINANCE

As explained in the introduction, the centre dominance picture applied directly to Wilson loops has been shown to be quantitatively successful, indeed in very good agreement with the full values [7]. In this approach any Wilson loop obtained from Monte Carlo results in SU(2) is approximated by its sign. It should be pointed out that in a weak sense it is not surprising that this reflects aspects of the dynamics: if one divides  $\rho(W_0)$  into odd and even parts, only the odd parts can contribute to  $\langle W_0 \rangle$  because that comes from the first moment of the distribution. We shall return to this point below. The result that the sign *alone* contains the essential dynamics is stronger and deserves examination.

In terms of the distribution, the centre dominance picture requires that we count  $-1$  for a loop with  $-\pi \leq \phi \leq 0$  and  $+1$  for  $0 \leq \phi \leq \pi$  with  $W_0 \equiv \sin(\phi/2)$ , i.e. a step distribution. We use the Fourier expansion of the Wilson loop distribution in eqn. (4) and obtain for the expectation value in this picture,

$$\begin{aligned} \langle W_0^{Z(2)} \rangle &= \int_0^\pi \rho \cos \frac{\phi}{2} \frac{d\phi}{2} - \int_{-\pi}^0 \rho \cos \frac{\phi}{2} \frac{d\phi}{2} \\ &= \frac{1}{2} \sum_n \left( \int_0^\pi b_n \sin n\phi \cos \frac{\phi}{2} d\phi - \int_{-\pi}^0 b_n \sin n\phi \cos \frac{\phi}{2} d\phi \right) = \sum \frac{nb_n}{n^2 - 1/4}. \end{aligned} \quad (16)$$

The series here is to be compared with the exact value  $\pi b_1/4$ . The important difference is the presence of all the higher  $b_n$ , with decreasing coefficients, in the centre dominance formula; without these the results would differ only by an overall factor of  $3\pi/16$ , which vanishes in the ratios required for the heavy quark potential (see eqn. (28), below). Why the value in eqn. (16) gives the correct value can therefore be clarified by looking at the values of  $b_n$  in the real distribution. Some support for this result is given by the uncorrelated loop picture, eqn. (14), where in doubling the area of a loop the new coefficients  $b_n$  are suppressed by a factor  $1/n$ , which in combination with the factor  $n/(n^2 - 1/4)$  in eqn. (16) shows that higher terms become progressively less important both for large  $A$  and for large  $n$ . If the other  $b_n$  are already smaller than  $b_1$  for small loops this effect is enhanced because of the powers of  $b_n$  involved.

We have calculated the coefficients  $b_n$  by binning Wilson loop data from Monte Carlo simulations and performing the integral for the Fourier coefficients,

$$b_n = \frac{1}{\pi} \int_{-\pi}^\pi \rho \sin n\phi d\phi, \quad (17)$$

numerically on the data at the end of the run. Errors have been estimated by averaging over values of  $b_n$  obtained in this way from several runs. The results here use 500 bins; we have compared this with the result from 200 bins in order to check that the discretisation error due to the finite number of bins is small. This error increases with the coefficient  $n$  as usual when sampling higher frequencies.

In fig. 4, we show the magnitude of the ratios of the second and third odd Fourier coefficients to the first, i.e.  $|b_2/b_1|$  and  $|b_3/b_1|$ , plotted against the area of the Wilson loop, for a  $12^4$  lattice at  $\beta = 2.5$ . Clearly, even  $b_2$  is negligible compared with  $b_1$  for loops larger than  $2 \times 2$ ;  $b_3$  disappears even faster;  $b_4$ , not shown, is smaller still. Thus the  $b_1$  term is the only one contributing to the centre dominance result, eq. (16), for loops of even moderate size and hence the result is the same, up to a trivial normalisation factor, as that from the full Wilson loop for all medium and large loops.

We also show the same ratios using the uncorrelated loop approximation, for comparison. As we have used the value in the plaquette distribution as the starting point for the higher coefficients,



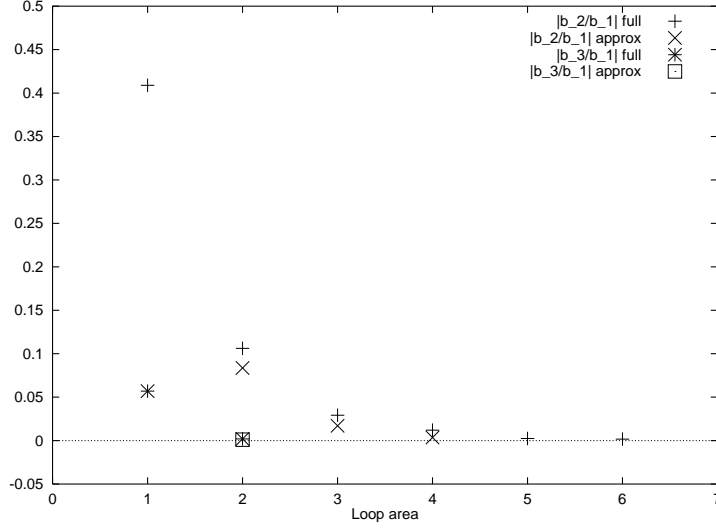


Figure 4: The ratios of the second and third coefficient in the Fourier expansion of the Wilson loop distribution to the first for small Wilson loops, plotted against the loop area in lattice units. Both the measured values and the uncorrelated loop predictions, normalised so that they are the same at unit area, are shown. Errors are negligible on this scale.

the points for area 1 are chosen to be the same as in the full case. However, the trend thereafter is similar, too. It has come from two places: first, the intrinsic behaviour of the model seen above, where higher  $b_n$  are more highly suppressed in larger loops; secondly, the fact that the initial coefficients  $b_n$  for higher  $n$  are already smaller and so powers of higher  $b_n$  disappear faster: only the first of the two is an explicit prediction of the model.

### *Behaviour in higher representations*

It turns out we are able to explain the results in the previous section as the effect of higher representation loops. As an alternative to eqn. (16), where we expanded the expectation value in the centre dominance picture in terms of Fourier coefficients, we could equally well have performed an expansion in terms of the characters of various representations; our conclusion would then have been that only the lowest half-odd-integer representation contributed for large loops. In fact, the expansions are the same up to constant factors.

To show this, we shall define the character of the representations in terms of the corresponding traces of the Wilson loop as

$$\chi_m(W_0) \equiv (m+1) \text{Tr}_{\frac{m}{2}} W, \quad (18)$$

where the representation has isospin  $m/2$ , so that the Tr operator is defined to contain the normalisation factor usually used in Monte Carlo calculations. The standard recurrence relation between the characters for SU(2) is

$$\chi_{m+1}(W_0) = \chi_m(W_0)\chi_1(W_0) - \chi_{m-1}(W_0). \quad (19)$$

We shall now show that using our variable  $\phi$ , defined in terms of the fundamental representation as  $\text{Tr}_{1/2} W \equiv W_0 \equiv \sin \frac{\phi}{2}$ , the characters for odd and even  $m$  can be written,

$$\begin{aligned} \chi_{2(n-1)}(W_0) &\equiv (-1)^{n-1} \frac{\cos(n - \frac{1}{2})\phi}{\cos \frac{\phi}{2}}, \\ \chi_{2n-1}(W_0) &\equiv (-1)^{n-1} \frac{\sin n\phi}{\cos \frac{\phi}{2}}. \end{aligned} \quad (20)$$

It is to be assumed that the value of the character at  $\phi = \pm\pi$  is found by taking the limit, although we have already noted that the distribution must vanish there from group-theoretic considerations. Note that  $\chi_0(W_0) \equiv 1$  and  $\chi_1(W_0) \equiv 2 \sin \frac{\phi}{2}$  as expected. Now we must prove that the following versions of eqn. (19) hold,

$$\begin{aligned}\chi_{2n}(W_0) + \chi_{2n-2}(W_0) &= \chi_{2n-1}(W_0)\chi_1(W_0), \\ \chi_{2n+1}(W_0) + \chi_{2n-1}(W_0) &= \chi_{2n}(W_0)\chi_1(W_0).\end{aligned}\tag{21}$$

This can easily be done by insertion of the formulae (20) into the respective left hand sides, whence standard trigonometric relations give the required results. Hence by induction the equations (20) are true for all  $n \geq 1$ .

Now we work out the expectation values of the traces using the distribution. For the representations with  $j = n - 1/2$ ,  $n \geq 1$ ,

$$\langle \text{Tr}_{n-\frac{1}{2}} W \rangle = \frac{1}{2n} \int_{-\pi}^{\pi} \rho(W_0) \chi_{2n-1}(W_0) \cos \frac{\phi}{2} \frac{d\phi}{2} = \frac{(-1)^{n-1} \pi b_n}{4n},\tag{22}$$

after inserting the Fourier expansion of eqn. (4) and the second of eqns. (20). Likewise for the representations  $j = n - 1$ ,  $n \geq 1$ , we have,

$$\langle \text{Tr}_{n-1} W \rangle = \frac{(-1)^{n-1} \pi a_n}{4(n-1/2)},\tag{23}$$

where  $n = 1$  and  $2$  correspond to the identity and adjoint representations respectively. Hence, as claimed, there is a one-to-one correspondence between the Fourier terms and the representations of the gauge group.

This means that the behaviour of the coefficients seen in fig. 4 is entirely consistent with the Casimir scaling hypothesis, recently discussed in the context of centre dominance [14], which notes that higher representations  $j = m+1/2$  have a string tension roughly proportional to the quadratic Casimir operator,

$$K_j \approx K_C \times j(j+1).\tag{24}$$

A larger string tension causes a stronger area law fall off, and hence from eqn. (22) the Fourier coefficients  $b_m$  decay faster in the loop area. Combined with eqn. (16), it can be seen that Casimir scaling implies centre dominance in the  $j = 1/2$  Wilson loops. This result would be rigorous if within Casimir scaling one included the assumption that all loops, not just those in the region of linear confinement, were suppressed by a similar factor. As the ratio of string tensions between  $j = 3/2$  and  $j = 1/2$  is already 5 in eqn. (24), it is not surprising that centre dominance holds so well.

Combining these results with the uncorrelated loop calculation in eqn. (14), we see that in the strong coupling limit all half-odd-integer representations have an area law behaviour similar to eqn. (15),

$$\langle \text{Tr}_{n-\frac{1}{2}} W(A) \rangle = \left( \frac{(-1)^{n-1} \pi b_n}{4n} \right)^A.\tag{25}$$

Indeed, we have also an area law in the integer representations,

$$\langle \text{Tr}_{n-1} W(A) \rangle = \left( \frac{(-1)^{n-1} \pi a_n}{4(n-\frac{1}{2})} \right)^A.\tag{26}$$

This is perhaps more of a surprise, as one often encounters the statement ‘strong coupling predicts a perimeter law behaviour in the adjoint representation’. The resolution of this is that the strong coupling expansion referred to in that statement is for a theory with the symmetry of the adjoint representation, in other words with an action that is restricted to an  $\text{SU}(2)/\text{Z}(2)$  symmetry. In

our case, however, the calculations are all performed with the fundamental SU(2) symmetry: the asymmetric appearance of the loop distributions, fig. 3, make this distinction clear. Indeed, one can measure loops in the adjoint representation in both fundamental or adjoint SU(2), and in the latter case, but not the former, a strong first order transition is found in Monte Carlo simulations, so it is quite clear the dynamics is different. As we have just shown, strong coupling predicts an area law behaviour in the former case; the question of whether such a string will break, due to shielding with gluons, is a different one again. One should therefore be careful of glib statements about the behaviour in the adjoint representation. We shall later return to the question of centre dominance in this case.

### *Centre projection and positive plaquettes*

In the last few years, detailed investigations of the importance of Z(2) degrees of freedom have been made by projecting the full SU(2) links to Z(2). One then makes plaquettes from these projected links, creating so-called projection vortices [4, 5]; a planar Wilson loop is simply a product of these over the minimal area.

As we have shown (see for example eqn. (6)), any observable contributing to the Wilson loop expectation value must come from the odd part of the distribution, so that it changes sign when the relevant loop does. It is natural to suppose the projection vortices are related, by some effect of the projection, to signs of Wilson loops, since that is where the effect of the centre appears physically. If this is the case, then the observation that no vortices means no area law is trivial: as we saw in discussing the loop distributions, no odd-sign behaviour means, in analytical terms, no contribution to the real expectation value. This does not mean that the relationship between the vortices and confining behaviour is trivial — the claim is that the physical string tension can be seen at particularly short distances in centre projection — merely that the presence of both positive and negative signs is necessary to observe the dynamics.

To make this a little clearer, consider the graphs showing the expectation value of Wilson loops separated according to whether they contain odd or even numbers of projection vortices in, for example, fig. 8 of ref. [4]: the Wilson loops separated in this way show no confining behaviour. Indeed, the fact that the Wilson loops go to zero at all is because the projection vortices do not exactly correspond to the signs of the full loops: suppose we look instead at the latter. As we have already seen, the distribution approaches (3) for large loops, and if we consider the part of the distribution with a positive value of the Wilson loop, we can see that large Wilson loops approach a constant value,

$$\langle |W_{0l}| \rangle = \int_{-1}^1 |W_0| \rho_l(W_0) dW_0 = \frac{2}{\pi} \int_{-1}^1 |W_0| (1 - W_0^2)^{1/2} dW_0 = \frac{4}{3\pi}, \quad (27)$$

and the negative loops taken alone correspondingly approach the limit  $-4/(3\pi)$ . This is a property of the even part of the distribution, unrelated to the odd part where  $\langle W_0 \rangle$  is to be found. (However, the adjoint string tension lives in the even part of the distribution: see below.)

The relationship between thick vortices and the sign of the loop is clearer in the positive plaquette model [9]. Here, plaquettes are constrained to have a positive value: this can be implemented by a simple accept/reject test in Monte Carlo updating. This model appears to have all the right properties to be an alternative lattice regularisation of SU(2) [10]. There are no thin vortices, which are simply lines of negative plaquettes, so that through the commutativity property of the centre any Wilson loop with a positive (negative) sign must contain an even (odd) number of thick vortices.

We have investigated the Wilson loop distribution in this theory, and show the results in fig. 5. The coupling here is  $\beta = 1.9$ , found to be in the scaling region for this theory [10]. The approach to the large loop region is, unsurprisingly, very similar to that shown in standard SU(2) in fig. 1.

The sign of the Wilson loop here counts thick vortices exactly and so the expectation values of Wilson loops with only even or odd numbers of thick vortices must tend to  $\pm 4/3\pi$ , irrespective of whether the vortices are responsible for the dynamics, i.e. irrespective of centre dominance. Our

point here is simply that one *must* consider loops with odd and even numbers of vortices together, as separately they can have no interpretation in terms of  $\langle W_0 \rangle$ .

We can also use the positive plaquette model to examine the question of whether the results from the  $Z(2)$  part agree with the full results when only thick vortices are present, or whether, on the other hand, both thick and thin vortices are required to produce the full result. Fig. 6 shows the potential between a heavy quark and an antiquark calculated from 150 configurations on a  $16^4$  lattice at  $\beta = 1.8$  for both the full results and those using only the signs of the Wilson loops. This figure corresponds to figures 7 and 8 of ref. [7] which show results in standard pure  $SU(2)$ ; our method is the same, i.e.  $V(R)$  is calculated from

$$V(R) = \lim_{T \rightarrow \infty} -\log \frac{W(R, T+1)}{W(R, T)} \quad (28)$$

with the signal improved by using fuzzing on spatial links only — this does not affect the presence of vortices in the  $(R, T)$  plane. To enable a comparison with the standard case we have also made a fit to the form

$$V(R) = V_0 + KR - e/R; \quad (29)$$

no correction for lattice artifacts has been made and the single correlated fit included all data with  $T \geq 3$  and  $R \geq 2.5$  for the full loops only (i.e. not using the  $Z(2)$  projected values). We obtained  $V_0 = 0.572(6)$ ,  $K = 0.0410(9)$  and  $e = 0.261(11)$ , corresponding to  $\beta$  slightly below 2.5 for standard  $SU(2)$ .

It is clear from fig. 6 that, as with standard  $SU(2)$  in ref. [7], the  $Z(2)$  part carries the physics; a similar picture (not shown) holds for  $\beta = 1.9$  where the curvature is more pronounced. Thus centre dominance is present across the whole size range, from the Coulomb to the confining region, works even with no thin vortices present. This is something of a relief, as the division into thin and thick vortices is an artifact of the cut-off. To see this, consider taking a negative plaquette, i.e. part of a thin vortex, and halving the lattice spacing: on the new lattice, it is no longer clear whether the loop corresponding to the former plaquette is (say) part of a thick vortex surrounding four positive plaquettes on the new lattice, or is negative by virtue of one of the those plaquettes being negative. In other words, the new lattice does not preserve the division into thin and thick vortices of the old one.

### *Confinement from non-interacting vortices*

We will show that a random distribution of non-interacting thick centre vortices, with no other dynamics, can give an area law in  $SU(2)$  with a string tension of about the right magnitude. This is the simplest possible treatment, although it is very much in the spirit of Nielsen–Olesen flux vortices [11, 12]; random vortices and their confining nature are not new and were considered for example in [13]. However it is now possible to make a quantitative test of the idea using results from centre vortices. A similar (but not identical) calculation appeared in ref. [14]; the version here has the advantage that it makes no reference to the lattice, even if the underlying assumptions are too simplistic for it to be a true continuum theory.

We assume that the value of a Wilson loop of area  $A$  depends only on the number of vortices inside, i.e.  $W_0(A) = W_C(-1)^n$ , where  $n$  vortices pass through the loop  $W_0$  and  $W_C$  depends only on the coupling: this is just the centre dominance proposal, which we have seen works well in practice. Although the assumption in this form does not fit in with the Wilson loop distributions we have shown, the proposal is that the sign alone determines the dynamics, so that the effect of the rest of the distribution on  $\langle W_0 \rangle$  can be absorbed into  $W_C$ .

We also assume that the vortices are independent from one another, so that any vortex can pass at a random point through a given area regardless of the presence of another: this second assumption is clearly an oversimplification, as there is indeed interaction between the vortices [16]. We are also assuming the vortices are infinitely thin, so that there are no edge effects; this, too, is

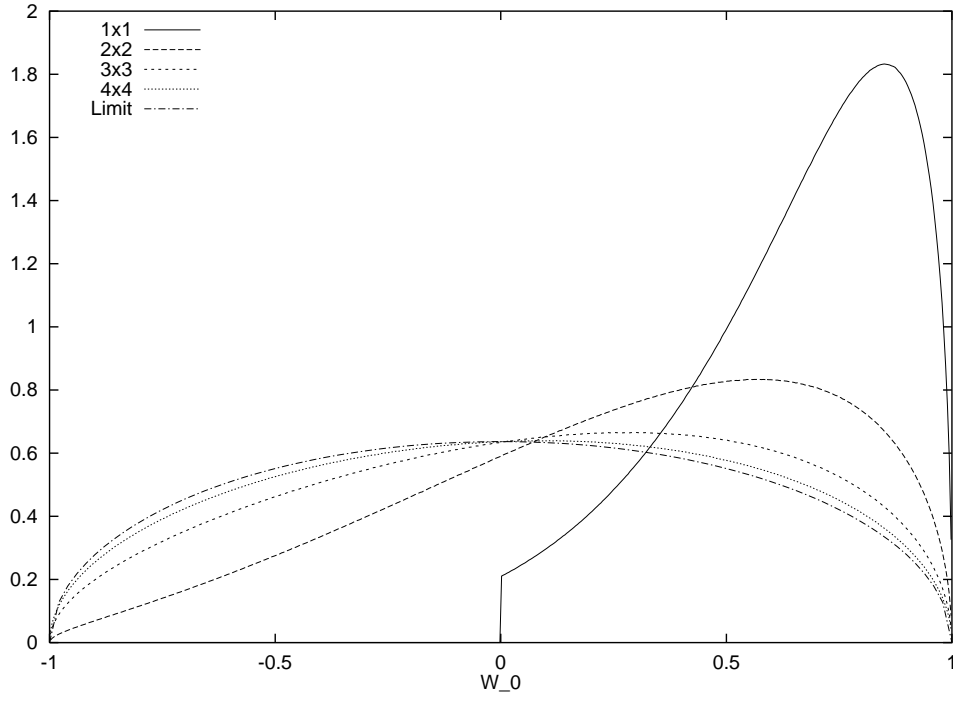


Figure 5: Monte Carlo distribution of Wilson loops on a  $12^4$  lattice at  $\beta = 1.9$  for the positive plaquette model, corresponding otherwise to figure 1.

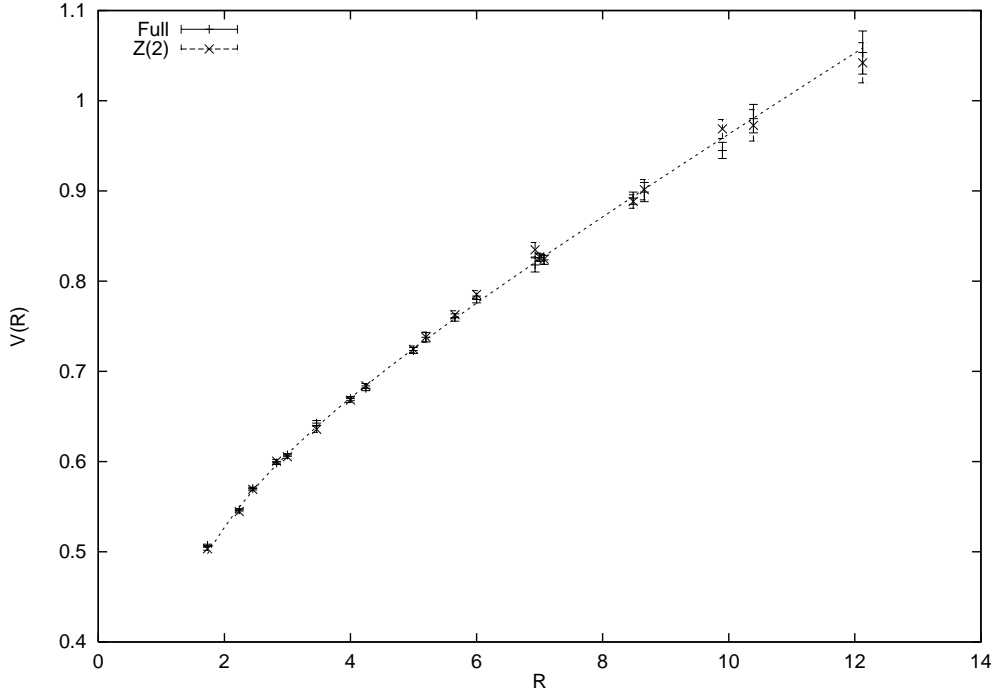


Figure 6: The heavy quark-antiquark potential from the positive plaquette model at  $\beta = 1.8$ , in lattice units. The dashed line is a three-parameter fit.

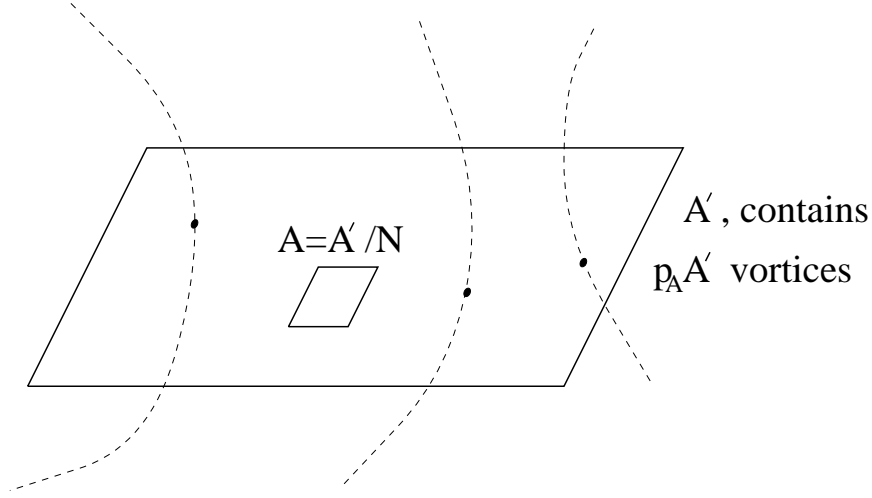


Figure 7: The random non-interacting vortex model, as described in the text.

unphysical, as we have already stressed that the vortices must be thick to survive in the continuum limit.

Finally, we suppose that the only relevant physical quantity is the mean density of vortices passing through unit area which we denote by  $p_A$ . In addition, we are using the fact of translational invariance so that there are equal probabilities for a vortex to pierce any regions with the same area. We are also essentially ignoring the fact that the vortices appear from the gauge dynamics.

Consider an area very much larger than  $A$ ,  $A' = AN$  for  $N \gg 1$ , which encloses  $A$  and through which exactly  $p_A A'$  vortices are assumed to pass, randomly distributed across the area: a three-dimensional slice is shown in fig. 7. For each vortex independently, there is a probability  $1/N$  that it lies inside  $A$ . The probability for  $n$  of them to lie in the area  $A$  is then given by a binomial distribution,

$$\Pr(n \text{ vortices in } A) = \binom{p_A A'}{n} \left(\frac{1}{N}\right)^n \left(1 - \frac{1}{N}\right)^{p_A A' - n}. \quad (30)$$

The contribution to the Wilson loop is

$$\langle W_0(A) \rangle = W_C \sum_{n=0}^{p_A A'} \binom{p_A A'}{n} (-1)^n \left(\frac{1}{N}\right)^n \left(1 - \frac{1}{N}\right)^{p_A A' - n} = W_C \left(1 - \frac{2}{N}\right)^{p_A AN}. \quad (31)$$

Letting  $N \rightarrow \infty$ , and noting that the limit as  $N$  tends to infinity of  $(1 - 2/N)^N$  is  $e^{-2}$ , we have

$$\langle W_0(A) \rangle = W_C e^{-2p_A A}, \quad (32)$$

which is an area law with string tension  $K = 2p_A$ . This result was obtained in a different approximation by ref. [6]; in this case we stress that its validity is based only on the notion of randomly distributed, non-interacting and (unfortunately) thin vortices.

A string tension of  $K = (440\text{MeV})^2$  would hence require  $p_A \approx 2.5 \text{ fm}^{-2}$ . Determining this quantity in a gauge invariant fashion is difficult, so we shall use the value calculated directly from  $Z(2)$ -projected vortices in ref. [15]:  $p_A = (1.9 \pm 0.2) \text{ fm}^{-2}$ , close to what we require. Further, the same value of the string tension was assumed in that calculation, so in fact the ratios of the two numbers are independent of the experimental value of  $K$ . Hence the random vortex model predicts a value of  $K$  about three quarters of the measured value (giving for  $\sqrt{K}$  some 85% of the measured value), the difference corresponding to three standard deviations. This is surprisingly

good considering the model in question contained very little mathematics and did not even take into account the extended nature of the vortices. That the centre vortices are physical is supported by the result of ref. [15] that the distribution is renormalisation group invariant.

### *The adjoint representation*

It has long been argued, and has to some extent entered the folklore, that the observation of a string tension in the adjoint representation of  $SU(2)$  cannot easily be explained by centre vortices. This claim is based on the point that the centre  $Z(2)$  of  $SU(2)$  is not seen by adjoint fields. This is, of course, correct, but this  $Z(2)$  is associated with *thin* centre vortices, which are not expected to be involved with confinement in the continuum limit — and as we saw from the positive plaquette model are not necessary even for lattice physics. The surviving symmetry of the adjoint representation is  $SU(2)/Z(2)$ , which is just that required for *thick* centre vortices. The mathematics of confinement relates to the fact that with  $SU(2)/Z(2)$  one has two types of path in the gauge manifold, one contractable and one not; the latter are closed due to the identification of opposite ends of a diameter of the manifold. This distinction survives in the adjoint representation.

In the adjoint representation, up to constants irrelevant to the argument, the action depends on the square of the plaquette value, and the negative trace of the loops is not seen. However, the fact that one cannot measure the signs of the loops in no way blurs the distinction between the topologically different windings of the field. One has simply lost a useful but — if the theory of thick centre vortices is correct — physically unnecessary label, namely the association between the sign of the loop and the presence of a vortex.

This last remark explains the difficulty with projection vortices, where factors of  $-1$  presumably correspond to a thick centre vortex with an increasing admixture of thin vortices for stronger coupling. Such vortices certainly are not present in the adjoint representation, making investigation of the mechanism considerably more difficult, but the underlying topology of the gauge manifold which forms the basis for confinement in the theory is still present.

The point made here is slightly different from the suggestion [14] for reconciling the adjoint string tension with the vortex picture involving sign flips. However, the finite width of the vortices enters in both cases: in that mechanism it was the origin of string behaviour in higher representations, while here we have stressed the  $SU(2)/Z(2)$  nature of the loops, which must be spread over a large area so as to be present in the continuum limit. Thus there may be a connection between the two.

We can show the correlations between the behaviour of adjoint Wilson loops and the presence of vortices directly. We have run a simulation on our  $12^4$  lattice at  $\beta = 2.5$  in which the adjoint loops are separated according to whether the fundamental loop was positive or negative, i.e. whether there is an even or odd number of vortices passing through the loop. This is just the process we criticised above for the fundamental case; however, here the sign of  $W_0$  itself is not seen by the adjoint trace,

$$W_0^{\text{adj}} = (4W_0^2 - 1)/3, \quad (33)$$

so that any correlation with the sign involves the  $SU(N)/Z(N)$  topology associated with the thick vortices. Indeed, the adjoint loop probes the even part of the distribution  $\rho(W_0)$  whereas, as we have made clear, the expectation values of fundamental loops and their signs only involve the odd part.

In fig. 8, we show the logarithms of the adjoint Wilson loops, both for the complete data and those with positive fundamental trace, once more at  $\beta = 2.5$ . There is clear sign of an area law behaviour in the former, i.e. an adjoint string tension. The latter have a consistently shallower gradient, in other words the string tension is significantly lower in those loops with only even numbers of vortices. A perfect or near-perfect correlation is not to be expected since from eqn. (33) that would require all loops with  $W_0 < 0$  also to have  $|W_0| < 1/4$ , and the other way around for positive  $W_0$ .

Phenomenologically, the source of the correlation is not hard to see from the fundamental distribution in fig. 1, bearing in mind that the expectation value we want is just eqn. (33) integrated

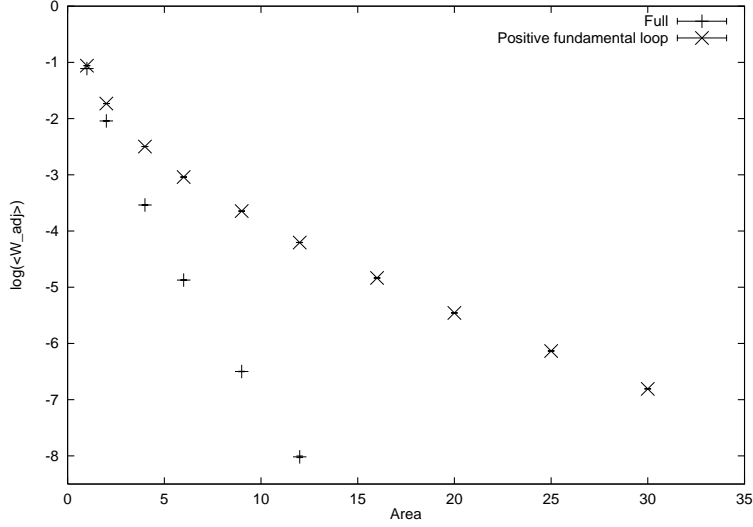


Figure 8: Logarithms of adjoint Wilson loops plotted against area. Both the complete data, and those loops associated with a positive fundamental loop, are shown.

over this distribution. For smaller loops, the distribution peaks at positive  $W_0$  and tails off towards negative values. Therefore, large absolute values of  $W_0$ , and hence positive contributions to  $W_0^{\text{adj}}$ , tend to come predominantly from positive fundamental loops. However, the source of the adjoint string tension itself is rather less easy to fathom by this method, and for that we appeal to the strong coupling result of eqn. (26) with  $n = 2$ .

As this work was being completed, ref. [17] appeared, showing similar correlations between the presence of vortices and the adjoint string tension.

## 5 SUMMARY

The major results of this paper are as follows:

- We considered the distribution  $\rho(W_0)dW_0$  of Wilson loops in SU(2); for loops larger than the correlation length of the field  $\rho(W_0)$  reaches the limiting form  $(2/\pi)\sqrt{1-W_0^2}$ .
- We applied the Fourier decomposition in eqn. (4); the expectation value of the loop is  $\langle W_0 \rangle = \pi b_1/4$ , in other words it only probes the first odd coefficient of the distribution in this parametrisation; the even portions of  $\rho(W_0)$  do not contribute.
- In the simple approximation where all Wilson loops are uncorrelated, and we use the measured plaquette distribution as input, the coefficient  $b_1$  and hence  $\langle W_0 \rangle$  obey the strong coupling behaviour, eqn. (15). Larger coefficients  $b_n$  are suppressed by an additional factor  $1/n$  for each multiplication by a Wilson loop of the same size. This approximation also shows an area law behaviour for the adjoint representation.
- The Z(2) expectation value contains all  $b_n$ , not just  $b_1$ . We found that for  $n > 2$  the coefficients were strongly suppressed in Monte Carlo results, showing the validity of centre dominance.
- The Fourier terms correspond, term by term, with the expectation value of the Wilson loop in the gauge group representations. The faster decay of higher representation loops therefore gives an explanation for centre dominance.



- We stressed that care needs to be taken when looking at results in  $Z(2)$ -projection (whether the links are projected or we simply look at the sign of the loops): the expectation values of the negative and positive parts separately are trivially seen to be non-confining, from the basic properties of the distribution.
- We showed by considering the positive plaquette model that the absence of thin vortices, which are chains of negative plaquettes, does not change the centre dominance behaviour.
- We showed that even a simple physical model of a random gas of centre vortices with no interactions gave three quarters of the observed string tension from the measured vortex density.
- We pointed out that there is no essential difficulty in having *thick* centre vortices explain an adjoint string tension, as both the thick vortices and the adjoint representation are associated with an  $SU(N)/Z(N)$  symmetry — the theory of centre dominance does not directly involve the centre  $Z(N)$ , as has sometimes been incorrectly assumed.
- We showed that there is a correlation between the adjoint string tension and the sign of the corresponding fundamental Wilson loop, even though the latter does not directly affect the adjoint loop: this makes it plausible that thick vortices are involved here, too. This correlation is easily seen by looking at the Wilson loop distributions.

These results seem to show that there is indeed physics contained in the centre dominance picture. However, it is important to ask what is the underlying physics. A lot of physics has also emerged from the maximally Abelian monopole condensation (Abelian dominance, or dual superconductor vacuum) picture [18]; see e.g. the proceedings of Lattice '97 [19] for recent progress. A way in which Abelian monopoles might be related to centre vortices has been proposed [5]. It is interesting to note that both models are based on topological mechanisms using homotopy classes, those of  $SU(2)/Z(2)$  or  $U(1)$ , not manifest in the full gauge group, and one can speculate that there is a deeper connection.

For further progress, one needs a better way of asking which properties are the most fundamental. Work is currently in progress by another group to try to understand the correlations between the monopole picture and instanton effects [20]; centre dominance is presumably another ingredient which needs to be taken into account. How far our results here really reflect dynamics involving the centre of the gauge group can presumably be clarified by looking at  $SU(3)$ .

## REFERENCES

- [1] J.M. Cornwall, Nucl. Phys. B157 (1979) 442.
- [2] G. 't Hooft, Nucl. Phys. B153 (1979) 141.
- [3] G. Mack and V.B. Petkova, Ann. Phys. (NY) 123 (1979) 442;(1979); *ibid.*, 125 (1980) 117; Z. Phys. C12 (1982) 177.
- [4] L. Del Debbio, M. Faber, J. Greensite and Š. Olejník, Phys. Rev. D55 (1997) 2298, hep-lat/9610005.
- [5] L. Del Debbio, M. Faber, J. Greensite and Š. Olejník, talk at the NATO Workshop “New Developments in Quantum Field Theory”, June 1997, Zakopane, Poland, hep-lat/9708023.
- [6] L. Del Debbio, M. Faber, J. Giedt, J. Greensite and Š. Olejník, hep-lat/9801027.
- [7] Tamás G. Kovács and E.T. Tomboulis, Phys. Rev. D57 (1998) 4054, hep-lat/9711009; Nucl. Phys. B (Proc Suppl.) 63 (1998) 534, hep-lat/9709042.
- [8] G. Bali, C. Schlichter and K. Schilling, Phys. Rev. D51 (1995) 5165, hep-lat/9409005.

- [9] G. Mack and E. Pietarinen, Nucl. Phys. B205 [FS5] (1982) 141.
- [10] J. Fingberg, U.M. Heller and V. Mitryushkin, Nucl. Phys. B435 (1995) 311, hep-lat/9407011.
- [11] H. Nielsen and P. Olesen, Nucl. Phys. B61 (1973) 45
- [12] H. Nielsen and P. Olesen, Nucl. Phys. B160 (1979) 380.
- [13] P. Olesen, Nucl. Phys. B200 [FS4] (1982) 381.
- [14] M. Faber, J. Greensite and S. Olejník, Phys. Rev. D57 (1998) 2603, hep-lat/9710039.
- [15] Kurt Langfeld, Hugo Reinhardt and Oliver Tennert, Phys. Lett. B419 (1998) 317, hep-lat/9710068.
- [16] M. Engelhardt, K. Langfeld, H. Reinhardt and O. Tennert, hep-lat/9801030.
- [17] M. Faber, J. Greensite and Š. Olejník, hep-lat/9807008.
- [18] G. 't Hooft, in EPS Conference on High Energy Physics, Palermo 1975, A. Zichichi, ed.; S. Mandelstam, Phys. Rep. 23C (1976) 245; G. Parisi, Phys. Rev. D11 (1975) 971.
- [19] Topology and Confinement parallel session, proceedings of Lattice '97, C.T.H Davies, I.M. Barbour, K.C. Bowler, R.D. Kenway, B.J. Pendleton and D.G. Richards, eds., Nucl. Phys. B (Proc Suppl.) 63 (1998) 465.
- [20] E.-M. Ilgenfritz, H. Markum, M. Müller-Preussker, W. Sakuler and S. Thurner, hep-lat/9804031.